Emissive Siloles

DOI: 10.1002/ange.200903698

Structural Modulation of Solid-State Emission of 2,5-Bis(trialkylsilylethynyl)-3,4-diphenylsiloles**

*Zujin Zhao, Zhiming Wang, Ping Lu, Carrie Y. K. Chan, Dandan Liu, Jacky W. Y. Lam, Herman H. Y. Sung, Ian D. Williams, Yuguang Ma, and Ben Zhong Tang**

Development of efficient luminescent materials is a topic of current interest. Understanding and manipulation of their light-emitting behaviors and performances in the solid state is of great importance because the materials are commonly used as thin films in their real-world applications.[1] In the solid state, the luminogenic molecules are located in close vicinity and are inclined to form aggregates. Chromophore aggregation can quench light emission, as short-range intermolecular interactions favor the formation of such detrimental species as excimers.[2] Besides this negative effect, aggregation can positively restrict intramolecular rotation (IMR), which rigidifies molecular conformations and blocks nonradiative decay channels.[3] Whether the aggregation weakens or strengthens light emission is decided by the competition between these two antagonistic physical effects, which is internally determined by the chemical structures of the luminogenic molecules.[4]

In our previous studies, we found that the positive effect prevails in propeller-shaped molecules, such as hexaphenylsilole (HPS) and tetraphenylethylene.[3] These molecules are non-emissive in solutions because of the active IMR processes of their multiple rotors but are induced to luminesce by aggregate formation owing to the restriction of their IMR processes in the condensed phase. These molecules have been referred to as "aggregation-induced emission" (AIE) luminogens. To enlarge the family of AIE luminogens and to gain insight into their structure–property relationships, herein we synthesized a group of new silole derivatives with systematically varied substituents at the 1,1- and 2,5-positions and studied how molecular structure, especially steric effects, of the substituents affect the packing arrangements and emission behaviors of the luminogens in the solid state.

The synthetic routes to the silole derivatives are presented in Scheme 1.[5,6] The key intermediate 2,5-dibromosiloles (**3**) were prepared by bromination of **2** with NBS. Cross-coupling

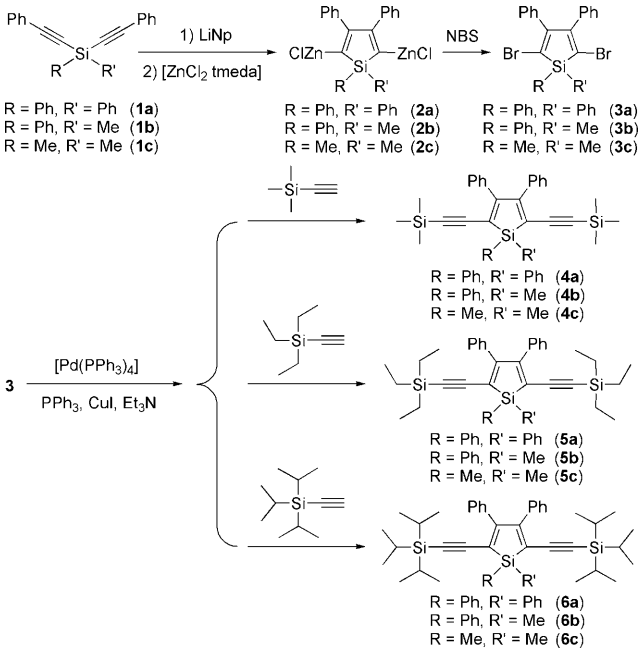

Scheme 1. Synthesis of silole derivatives. Np = naphthyl, tmeda = *N*,*N*,*N*′,*N*′-tetramethylethylenediamine, NBS = *N*-bromosuccinimide.

of **3** with alkynes gave the target products (**4**–**6**) in high yields (83–95%). The detailed synthetic procedures and characterization data are given in the Supporting Information. Single crystals of **4a**, **5a**, **5c**, and **6a**–**c** were grown from their THF/methanol solutions and analyzed by X-ray diffraction crystallography. The crystal structures of the silole derivatives are shown in Figure 1, and their detailed crystal analysis data are given in Tables S1 and S2 in the Supporting Information.

The energy levels of the highest occupied and lowest unoccupied molecular orbitals (HOMO and LUMO) of **4**–**6** were calculated using the B3LYP/6-31G* basis set. The data are summarized in Tables S3–S5 and Figure S1 in the Supporting Information, and those for **6a** are plotted in Figure 1 as an example. The orbitals are dominated by the contributions from the silole rings and the 2,5-ethynyl triple bonds, thanks to their orbital overlap and electronic commu-

[*] Dr. Z. Zhao, Dr. P. Lu, C. Y. K. Chan, Dr. J. W. Y. Lam, Dr. H. H. Y. Sung, Prof. Dr. I. D. Williams, Prof. Dr. B. Z. Tang
Department of Chemistry, The Hong Kong University of Science & Technology
Clear Water Bay, Kowloon, Hong Kong (China)
Fax: (+852) 2358-1594
E-mail: tangbenz@ust.hk
Homepage: http://home.ust.hk/~tangbenz/
Z. Wang, D. Liu, Prof. Dr. Y. Ma
State Key Laboratory of Supramolecular Structure and Materials
Jilin University, Changchun 130012 (China)

[**] We thank the Research Grants Council of Hong Kong (603008 and 601608), the Ministry of Science & Technology of China (2009CB623605) and the National Science Foundation of China (20634020). B.Z.T. is grateful to Cao Gaungbiao Foundation of Zhejiang University.

Supporting information for this article is available on the WWW under http://dx.doi.org/10.1002/anie.200903698.

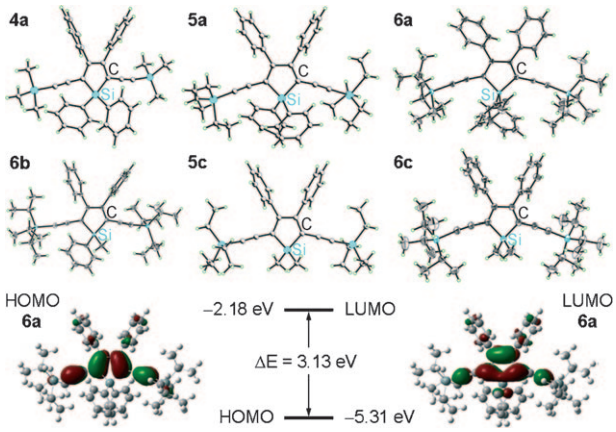

Figure 1. Molecular structures of **4a**, **5a**, **6a**, **6b**, **5c**, and **6c** (see the Supporting Information for detailed crystal analysis data) and molecular orbital amplitude plots of HOMO and LUMO energy levels of **6a** calculated using the B3LYP/6-31G* basis set (see the Supporting Information for the plots for other silole derivatives).

nication. The HOMO energy levels of the silole derivatives are located in the range of −5.28 to −5.31 eV, comparable to that of dimethyltetraphenylsilole (DMTPS; −5.29 eV).[7] Their LUMO energy levels, however, are from −2.10 to −2.18 eV, lower than that of DMTPS (−1.59 eV), thus indicating that these new silole derivatives have higher electron affinities.

Dilute THF solutions of **4**–**6** show absorption peaks (λ_{ab}) at approximately 400 nm, which arise from the π–π* transition of the 2,5-diethynylsilole moiety (Table 1). Changing the 1,1-substituents from two methyl groups to one methyl and one phenyl to two phenyl groups progressively red-shifts the λ_{ab} of the silole derivatives, owing to the gradually strengthened inductive effect.[5] The silole solutions emit weakly, because their active IMR processes annihilate the excitons. Their fluorescence quantum yields (Φ_F) are low (0.32–1.67%), but are somewhat higher than that of HPS (0.1%),[6] owing to their more conjugated electronic structures.

Table 1: Absorption and emission characteristics of silole derivatives **4**–**6** in solution, amorphous, and crystalline states[a]

Silole	λ_{ab} [nm]	λ_{em} [nm]			Φ_F [%]	
	Soln	Soln	Amor	Cryst	Soln[b]	Amor[c]
4a	400	485	518	520	0.75	26.8
4b	397	486	542		0.41	33.3
4c	393	486	544		0.32	26.1
5a	403	488	486	496	1.03	39.9
5b	398	486	524		0.46	76.4
5c	394	484	535	536	0.24	62.6
6a	403	491	484	495	1.67	76.6
6b	399	488	489	501	0.74	99.9
6c	396	489	481	498	0.39	57.1

[a] Abbreviations: Soln = solution (10 μM in THF), Amor = amorphous, Cryst = crystal, λ_{ab} = absorption maximum, λ_{em} = emission maximum, Φ_F = fluorescence quantum yield. [b] Estimated using 9,10-diphenylanthracene (Φ_F = 90% in cyclohexane) as the standard. [c] Measured using an integrating sphere.

Similar to HPS, the silole derivatives become stronger emitters when they are aggregated. As can be seen from the example shown in Figure 2a, the emission of **4b** is intensified when a large amount of water ($f_w > 70\%$) is added into THF.

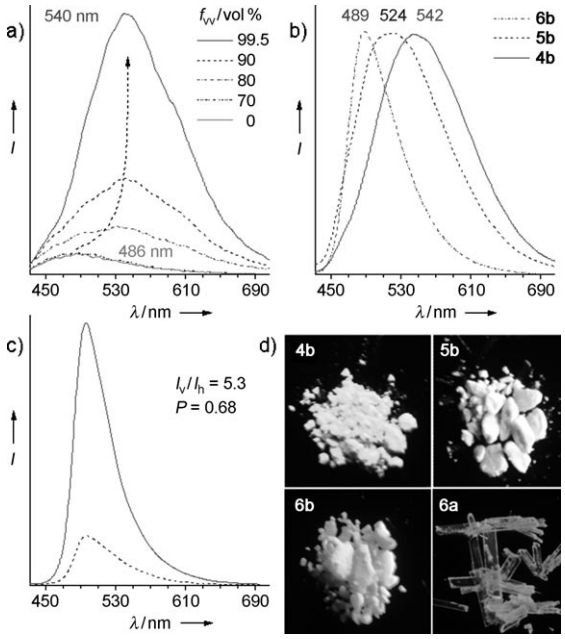

Figure 2. a) Emission spectra of **4b** in THF/water mixtures with different fractions of water (f_w). b) Emission spectra of amorphous powders of **4b**, **5b**, and **6b**. c) Polarized emission spectra of crystals of **6a**; excitation wavelength: 370 nm; I_v = intensity in vertical direction (——), I_h = intensity in horizontal direction (-----), P = degree of polarization [$P = (I_v - I_h)/(I_v + I_h)$]. d) Photographs of the powders of **4b**, **5b**, and **6b** and the crystals of **6a** taken under UV illumination.

The higher the water content, the stronger the light emission. Since water is a nonsolvent of **4b**, the silole molecules must have aggregated in the aqueous mixtures with high water contents. This result verifies that the silole emission is enhanced by aggregate formation. High water content populates the silole aggregates, thereby boosting the light emission. A similar emission-enhancement effect is observed in other silole systems, thus revealing that the silole derivatives are all AIE luminogens.

The nice results obtained from the aggregates suspended in aqueous media prompted us to further study the silole emissions in the solid state. The amorphous powders of **4b**, **5b**, and **6b** fluoresce at 542, 524, and 489 nm (Figure 2b) in efficiencies of 33.3, 76.4, and 99.9% (Table 1), respectively. A similar trend is observed in the series of **4a**→**5a**→**6a** and **4c**→**5c**→**6c** (Table 1). Evidently, when 2,5-substituents in a silole molecule become bulkier (methyl→ethyl→isopropyl), its emission color (λ_{em}) is hypsochromically shifted (Figure 2d) and its emission efficiency (Φ_F) is generally enhanced.

It is worth noting that the silole molecules with dissimilar 1,1-substituents always stand out and show the highest Φ_F values among their congeners: for example, in the family of **6a**–**c**, **6b** exhibits the highest emission efficiency (99.9%). This finding is similar to what we have observed in other AIE

systems: the silole molecules with different 1,1-substitutions display higher Φ_F values, because they are difficult to pack compactly in the solid state, and their excitons are less likely to be quenched by intermolecular interactions.[3]

In our previously studied silole systems, aggregate formation dramatically boosted the emission efficiency but caused little shift in the emission color in comparison to the data for dilute solution.[3] In contrast, the emission colors of **4**–**6** vary with aggregate formation (Table 1). The emission maximums (λ_{em}) for amorphous powders of **4** and **5** are generally red-shifted from those of their solutions (e.g., $\Delta\lambda_{em} = +58$ nm for **4c**), while the opposite effect is observed in the system of **6** (e.g., $\Delta\lambda_{em} = -8$ nm for **6c**). Another difference is that the λ_{em} values for the amorphous powders of **4** and **5** are red-shifted in the order of **a**→**b**→**c** (cf. $\lambda_{em} =$ 518 nm for **4a**, $\lambda_{em} = 544$ nm for **4c**), but those in the system of **6** are generally blue-shifted (cf. $\lambda_{em} = 484$ nm for **6a**, $\lambda_{em} =$ 481 nm for **6c**).

We further investigated the emission behaviors of the aggregates of **4**–**6** in the crystalline state. Compared to their isolated species in the dilute solutions, the crystals of the silole derivatives all emit further into the red spectral region. The extent of the spectral shift varies with the molecular structure. For example, the crystals of the silole dye carrying smaller trimethylsilyl substituents (**4a**) furnish a λ_{em} of 520 nm, which is 35 nm red-shifted from the corresponding value in solution. The silole derivatives bearing larger triisopropylsilyl groups (**6**) display much smaller red shifts when they are crystallized. This finding suggests that the bulky 2,5-substituents help reduce intermolecular interactions. The light emissions of the crystals of **4**–**6** are also influenced by the 1,1-substitutions. The phenyl group works better in terms of suppressing intermolecular interactions than the methyl group because of the larger size of the aromatic ring. This property is manifested by the crystal emissions of **5a** and **5c**: the former emits at 496 nm, while the latter emits at 536 nm.

In an effort to understand the mechanism operating in the AIE system, we checked geometric structures and packing arrangements of the silole molecules in the crystalline state. As can be seen from the example shown in Figure 3a, a C–H···π hydrogen bond ($d_1 = 3.077$ Å) is formed between a hydrogen atom of the trimethylsilyl group in one molecule of **4a** and the π electron cloud of a phenyl ring in another molecule. A C–H···π hydrogen bond ($d_2 = 2.749$ Å) is also formed between two phenyl rings in neighboring molecules. These multiple C–H···π hydrogen bonds help rigidify the molecular conformation and restrict IMR processes, thus making the crystals of **4a** highly emissive. During crystallization, the silole molecules may adjust their conformations to fit into the crystalline lattices, and the silole core and 2,5-ethynyl rods may become more coplanar. The planarized silole molecules possess better electronic conjugation and experience stronger intermolecular interactions in the crystal cells, thereby causing the silole emission to red shift.

On the other hand, the steric effects of the bulky triisopropylsilyl substituents give rise to wide separation between the molecules in the crystal structure, as evidenced by the large interplane distance ($d_3 = 6.629$ Å) between the ethynyl rods in two neighboring molecules of **6a** (Figure 3b). This situation leads to weakened intermolecular interactions and accounts for the smaller red shift of the crystal emission from the solution emission ($\Delta\lambda_{em} = 4$ nm). The molecules of **6a** are stuck in an antiparallel fashion in the crystal lattice (Figure 3c), which effectively restricts IMR processes and dramatically boosts the emission efficiency.

Orderly packed molecules in the solid state can emit polarized light. Polarized emission, however, is often quenched in "conventional" luminophoric materials owing to strong π stacking interactions in their solids. Thanks to the unique AIE nature, **4**–**6** emit intensely in the condensed phase. Remarkably, their crystals display emission anisotropy, with stronger emission in the vertical direction. The polarized emission spectra for the crystals of **6a** are shown in Figure 2c. The ratio of emission intensities (I_v/I_h) and the degree of polarization (P) are 5.3 and 0.68, respectively. These values are rather high, close to those for single-crystal nanorods of CdSe, a highly emissive inorganic semiconductor.[8] While crystals cannot be grown from the solution of **4c**, it readily forms microfibers on a quartz plate. The microfibers emit green, yellow, and red light when excited at different wavelengths (Supporting Information, Figure S2), thus realizing multiple color emissions from one luminogenic molecule by simply changing the excitation wavelength.

In summary, we have synthesized a group of silole derivatives with systematically varying 1,1- and 2,5-substituents. The solid-state emissions of the luminogens are found to be tunable by changing the molecular structure, especially the steric effects, of the substituents. Bulkier substituents help weaken the intermolecular interactions and restrict the IMR process, thereby blue-shifting the emission color and dramatically boosting the emission efficiency (Φ_F up to 99.9%). Polarized and multicolor emissions are realized in silole crystals and fibers, respectively. The information gained in this work on the structure–property relationships in the AIE system is of great value in terms of guiding our future molecular engineering endeavors in designing molecular structures for new luminogenic materials with desired light-emitting properties in the solid state.

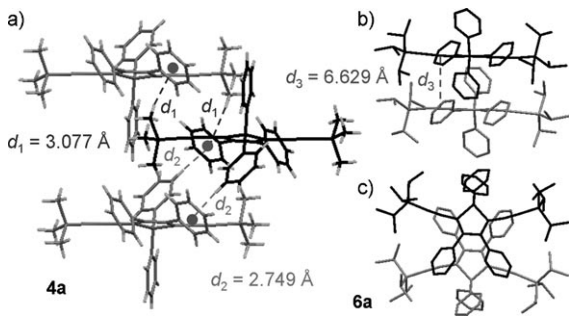

Figure 3. a) Packing arrangement in the crystal structure of **4a**, with C–H···π hydrogen bonds marked by dashed lines. b) Top and c) side views of adjacent molecules of **6a** in its crystal structure.

Received: July 7, 2009
Published online: September 4, 2009

Keywords: aggregation-induced emission · fluorescence · luminescence · siloles · structure–activity relationships

[1] a) A. C. Grimsdale, K. L. Chan, R. E. Martin, P. G. Jokisz, A. B. Holmes, *Chem. Rev.* **2009**, *109*, 897; b) J. W. Y. Lam, B. Z. Tang, *Acc. Chem. Res.* **2005**, *38*, 745.

[2] a) M. Shimizu, K. Mochida, T. Hiyama, *Angew. Chem.* **2008**, *120*, 9906; *Angew. Chem. Int. Ed.* **2008**, *47*, 9760; b) Y. Dong, J. W. Y. Lam, A. Qin, Z. Li, J. Sun, Y. Dong, H. H. H. Sung, I. D. Williams, B. Z. Tang, *Chem. Commun.* **2007**, 40; c) S. J. Lim, B. K. An, S. D. Jung, M. A. Chung, S. Y. Park, *Angew. Chem.* **2004**, *116*, 6506; *Angew. Chem. Int. Ed.* **2004**, *43*, 6346; d) S. Yin, Q. Peng, Z. Shuai, W. Fang, Y. Wang, Y. Luo, *Phys. Rev. B* **2006**, *73*, 205409; e) Y. Dong, J. W. Y. Lam, A. Qin, Z. Li, J. Sun, Y. Dong, B. Z. Tang, *J. Inorg. Organomet. Polym. Mater.* **2007**, *17*, 201; f) B.-K. An, S.-K. Kwon, S.-D. Jung, S. Y. Park, *J. Am. Chem. Soc.* **2002**, *124*, 14410; g) T. Ozdemir, S. Atilgan, I. Kutuk, L. T. Yildirim, A. Tulek, M. Bayindir, E. U. Akkaya, *Org. Lett.* **2009**, *11*, 2105.

[3] a) Y. Hong, J. W. Y. Lam, B. Z. Tang, *Chem. Commun.* **2009**, 4332; b) G. Yu, S. Yin, Y. Liu, J. Chen, X. Xu, X. Sun, D. Ma, X. Zhan, Q. Peng, Z. Shuai, B. Z. Tang, D. Zhu, W. Fang, Y. Luo, *J. Am. Chem. Soc.* **2005**, *127*, 6335; c) J. Luo, Z. Xie, J. W. Y. Lam, L. Cheng, H. Chen, C. Qiu, H. S. Kwok, X. Zhan, Y. Liu, D. Zhu, B. Z. Tang, *Chem. Commun.* **2001**, 1740.

[4] a) X. Fang, J. Sun, F. Wang, Z. Chu, P. Wang, Y. Dong, R. Hu, B. Z. Tang, D. Zou, *Chem. Commun.* **2008**, 2989; b) J. Liu, J. W. Y. Lam, B. Z. Tang, *J. Inorg. Organomet. Polym. Mater.* **2009**, *19*, 249.

[5] a) K. Tamao, S. Yamaguchi, M. Shiro, *J. Am. Chem. Soc.* **1994**, *116*, 11715; b) S. Yamaguchi, K. Iimura, K. Tamao, *Chem. Lett.* **1998**, 89; c) A. J. Boydston, Y. Yin, B. L. Pagenkopf, *J. Am. Chem. Soc.* **2004**, *126*, 10350; d) A. J. Boydston, Y. Yin, B. L. Pagenkopf, *Angew. Chem.* **2004**, *116*, 6496; *Angew. Chem. Int. Ed.* **2004**, *43*, 6336; e) S. Yamaguchi, R. Z. Jin, K. Tamao, *J. Organomet. Chem.* **1998**, *559*, 73; f) S. Yamaguchi, K. Tamao, *J. Chem. Soc. Dalton Trans.* **1998**, 3693; g) M. Katkevics, S. Yamaguchi, A. Toshimitsu, K. Tamao, *Organometallics* **1998**, *17*, 5796.

[6] J. Chen, C. W. Law, J. W. Y. Lam, Y. Dong, S. Lo, I. D. Williams, D. Zhu, B. Z. Tang, *Chem. Mater.* **2003**, *15*, 1535.

[7] C. Risko, G. P. Kushto, Z. H. Kafati, J. L. Brédas, *J. Chem. Phys.* **2004**, *121*, 9031.

[8] J. Hu, L.-S. Li, W. Yang, L. Manna, L.-W. Wang, A. P. Alivisatos, *Science* **2001**, *292*, 2060.

